

***Saccharomyces cerevisiae* HMO1 interacts with TFIID and participates in start site selection by RNA polymerase II**

Koji Kasahara, Sewon Ki, Kayo Aoyama, Hiroyuki Takahashi and Tetsuro Kokubo*

Division of Molecular and Cellular Biology, International Graduate School of Arts and Sciences, Yokohama City University, Yokohama, 230-0045, Japan

Received October 11, 2007; Revised November 11, 2007; Accepted November 12, 2007

ABSTRACT

Saccharomyces cerevisiae HMO1, a high mobility group B (HMGB) protein, associates with the rRNA locus and with the promoters of many ribosomal protein genes (RPGs). Here, the Sos recruitment system was used to show that HMO1 interacts with TBP and the N-terminal domain (TAND) of TAF1, which are integral components of TFIID. Biochemical studies revealed that HMO1 copurifies with TFIID and directly interacts with TBP but not with TAND. Deletion of *HMO1* ($\Delta hmo1$) causes a severe cold-sensitive growth defect and decreases transcription of some TAND-dependent genes. $\Delta hmo1$ also affects TFIID occupancy at some RPG promoters in a promoter-specific manner. Interestingly, over-expression of HMO1 delays colony formation of *taf1* mutants lacking TAND (*taf1* Δ TAND), but not of the wild-type strain, indicating a functional link between HMO1 and TAND. Furthermore, $\Delta hmo1$ exhibits synthetic growth defects in some *spt15* (TBP) and *toa1* (TFIIA) mutants while it rescues growth defects of some *sua7* (TFIIB) mutants. Importantly, $\Delta hmo1$ causes an upstream shift in transcriptional start sites of *RPS5*, *RPS16A*, *RPL23B*, *RPL27B* and *RPL32*, but not of *RPS31*, *RPL10*, *TEF2* and *ADH1*, indicating that HMO1 may participate in start site selection of a subset of class II genes presumably via its interaction with TFIID.

INTRODUCTION

Transcriptional initiation of protein-coding (class II) genes by RNA polymerase II (Pol II) involves a set of general transcription factors (GTFs: TFIIA, TFIIB, TFIID, TFIIIE, TFIIF and TFIIH), as well as other cofactors including mediator, histone-modifying enzymes and ATP-dependent chromatin remodeling complexes (1–3).

Upon transcriptional activation, gene-specific activators recruit the active forms of these components to the promoter region surrounding the transcriptional initiation site of target genes (4,5). Despite considerable investigation, details of the molecular mechanisms underlying transcriptional activation remain unclear. TFIID, which is composed of the TATA box-binding protein (TBP) and 14 TBP-associated factors (TAFs), not only recognizes a set of core promoter elements, but also serves as one of the most important targets for activators (6). The TAF1 N-terminal domain, TAND, binds to the concave and convex surfaces of TBP, thereby inhibiting TBP binding to the TATA element (7). The loading of TBP onto the promoter is a key regulatory step for activation (8–10) and, thus, we proposed that activators reverse the TAND–TBP interaction, enabling formation of a productive TFIIA–TBP–TATA complex (11).

High mobility group B (HMGB) proteins constitute a subgroup of non-histone HMG proteins in eukaryotic chromatin. They contain one or more HMG box domains (12,13) that are distinctive DNA-binding motifs, in which the global fold is well conserved and comprises three helices arranged in an L-shape (14,15). HMGB proteins are involved in diverse biological processes, including transcription, recombination and DNA repair, by facilitating assembly of nucleoprotein complexes that are required for these processes (16–18). Notably, some yeast and human HMGB proteins are transcriptional coactivators that stabilize the TBP/TFIID–TFIIA–promoter complex (19,20).

Saccharomyces cerevisiae expresses seven HMGB proteins, HMO1, HMO2 (also called NHP10), NHP6A, NHP6B, ABF2, ROX1 and IXR1. Among these proteins, only HMO1 is involved in both RNA polymerase I (Pol I)- and Pol II-mediated transcription (21–23). HMO1 binds to promoters of most ribosomal protein genes (RPGs, 97 of 138) as well as promoters of 386 non-RP target loci over the entire genome (22,23). Our recent work also revealed that 138 RPGs can be classified into 13 distinct groups based on HMO1-abundance at the

*To whom correspondence should be addressed. Tel: +045 508 7237; Fax: +045 508 7369; Email: kokubo@tsurumi.yokohama-cu.ac.jp

promoter and the HMO1-dependence of FHL1 and/or RAP1 binding to the promoter (23). Both FHL1 and/or RAP1 are key regulators of RPG transcription (24–30). Interestingly, FHL1 binds to most of the HMO1-enriched and transcriptionally HMO1-dependent RPG promoters in an HMO1-dependent manner, whereas it binds to HMO1-limited RPG promoters in an HMO1-independent manner (23).

This study shows that HMO1 interacts physically and genetically with TAND and TBP/TFIID. Genetic analyses also indicate a close relationship between the functions of HMO1 and TAND, TBP, TFIIB and TFIIA. Surprisingly, $\Delta hmo1$ rescues growth defects of some *sua7* (TFIIB) mutants and causes an upstream shift in transcriptional start sites of some genes, e.g. *RPS5*, *RPS16A*, *RPL23B*, *RPL27B* and *RPL32*, but not of others, e.g. *RPS31*, *RPL10*, *TEF2* and *ADH1*. Similarly, *tfg1/tfg2* (TFIIF) (31–33) and *rpb2/rpb9* (Pol II) (34–37) mutations rescue the growth defect of some *sua7* mutants, and also shift the start site of *ADH1* upstream. Thus, it is likely that HMO1 participates in the start site selection of a subset of class II genes by a mechanism that differs from that of TFIIF and Pol II.

MATERIALS AND METHODS

Yeast strains

Standard techniques were used for growth and transformation of yeast (38). The yeast strains used in this study are listed in Supplementary Table 1. The $\Delta spt15$ strain (YTK271) has been described previously (39). YTK271, YTK8264, YTK8270, YTK8166, YTK8269 and YTK8273 were used as parental strains for exchange of plasmids encoding wild-type TBP, TFIIB or TFIIA with plasmids encoding mutant proteins. YKK74 was generated as described previously (23).

Targeted disruption of *HMO1* was performed by PCR-based gene deletion (40) using the primers TK4022 and TK4023. The oligonucleotides used in this study are listed in Supplementary Table 2. *HMO1* disrupted strains YTK8468, YTK8166, YTK8269 and YTK8273 were generated from Y13.2, YTK271, YTK8264 and YTK8270, respectively, using *HIS3* as the selectable marker. Using *kanMX* as the selectable marker, targeted disruptions of *SUA7* (primers TK7770-TK6225) and *TOA1* (primers TK7768-TK5565) were performed in the H2451 strain (41) to generate the YTK8264 and YTK8270 strains, respectively.

A number of strains were generated using a plasmid shuffle technique, whereby, for example, pYN1/*TAF1* (*URA3* marker) was replaced with a *TRP1*-marked plasmid, by growing transformants on 5-fluoroorotic acid (5-FOA)-containing plates. Using the plasmids pM2715/*TAF1*, pM2722/*taf1* Δ 2-86 or pM2727/*taf1* Δ 2-186, the YTK8472, YTK8473 and YTK8474 strains, respectively, were generated from YTK8468 and the YTK8469, YTK8470 and YTK8471 strains, respectively, were generated from Y13.2. YKK237, YKK238, YKK241 and YKK247 were generated from Y22.1 (41) using the pM1169/*TAF1*,

pM977/*taf1* Δ 41-73, pM1002/*taf1* Δ 8-42 or pM1001/*taf1* Δ 10-73 plasmids, respectively.

Construction of plasmids for the Sos recruitment system

A 0.65 kb fragment containing TAND (1–208 aa) was amplified by PCR using the TK2697 and TK2698 primers, and then ligated into a blunt-ended BamHI site in pSos (Stratagene), generating the bait plasmid pM2718. A 0.89 kb fragment containing the *GAL1* promoter, a myristylation signal and the *CYC1* terminator of pMyr (Stratagene) was amplified by PCR using the TK3528 and TK3529 primers, and ligated into the PvuII site of pRS426 (42), forming the pM2721 vector. As prey, yeast cDNA was prepared using a cDNA synthesis kit (Stratagene), digested with EcoRI-XhoI and then ligated into a similarly digested pM2721.

DNA fragments (0.73 kb) encoding TBP were amplified by PCR using the TK4348-TK936 primers, then digested and ligated into the BamHI-SalI sites of pSos, forming pM2875 or amplified using the TK21-TK936 primers, digested and ligated into the EcoRI-SalI sites of pMyr, forming pM2719. A 0.74 kb fragment encoding *HMO1* was amplified by PCR using the TK3807 and TK3808 primers, digested, and ligated into the EcoRI-XhoI site of pM2721, forming pM2754.

Construction of plasmids for the GST pulldown assay

The plasmid encoding His-TBP (pM1578) has been described previously (39). A 0.73 kb fragment encoding TBP was amplified by PCR using the TK1 and TK2 primers, digested, and ligated into the BamHI-EcoRI sites of pGEX-2T (GE Healthcare Biosciences), generating pM4673 (encoding GST-TBP). Similarly, the expression plasmids pM2773 (GST-TAND; 6–208 aa) and pM2823 (GST-HMO1, 1–246 aa) were constructed by ligating a 0.6 kb BamHI (internal)-NotI fragment from pM2718 and a 0.74 kb EcoRI-XhoI fragment from pM2754, respectively, into pGEX-6P-1 (GE Healthcare Biosciences). The expression plasmid pM5214 (His-HMO1) was constructed by ligating a 0.74 kb EcoRI-XhoI fragment from pM2754 into pCold 1 (TaKaRa).

Construction of plasmids for genetic studies

TAF1 plasmids. pM1169 (*TAF1*/pRS314), pM1001 (*taf1* Δ 10-73/pRS314), pM1002 (*taf1* Δ 8-42/pRS314), pM977 (*taf1* Δ 41-73/pRS314), pM1689 (*taf1* Δ 2-86/pRS314) and pM1657 (*taf1* Δ 2-186/pRS314) have been described previously (43,44). The NcoI-NruI fragment of pM1169 was replaced with the NcoI-EcoRV fragment of pBS1479, generating pM2711. A 0.82 kb fragment was amplified by PCR from pM1169 using the TK120 and TK3516 primers, digested and ligated into the NcoI site of pM2711, generating pM2715 (*TAF1-TAP*/pRS314). The 1.6 kb BlnI-PstI fragments of pM1689 and pM1657 were replaced with the BlnI-PstI fragment of pM2715, generating pM2722 and pM2727, respectively.

HMO1 plasmids. pM2897 was constructed by ligating a 0.74 kb EcoRI-XhoI fragment from pM2754 into similarly digested p414-TEF (45). SacI-NaeI fragments

from pM2897 (1.8 kb), pM2899 (2.05 kb), pM2933 (1.5 kb) and p414-GPD (1.3 kb) were ligated into similarly digested pRS315 (46), generating pM2949 (*TEF1* promoter-driven *HMO1*/pRS315), pM2950 (*TDH3* promoter-driven *HMO1*/pRS315), pM2956 (*TDH3* promoter-driven *VTC1*/pRS315) and pM2959 (*TDH3* promoter only/pRS315), respectively. pM2899 was constructed by ligating a 0.74 kb EcoRI-XhoI fragment from pM2754 into similarly digested p414-GPD (45). A 0.45 kb fragment encoding *VTC1* was amplified by PCR using the TK2340 and TK2341 primers, digested and ligated into the BamHI-PstI sites of p414-GPD, generating pM2933.

TBP, TFIIB and TFIIA plasmids. Plasmids expressing wild-type TBP or its mutants in yeast cells have been described previously (39). In this study, the following plasmids were generated to express TFIIB, TFIIA and their mutants. A 3.0 kb fragment containing *SUA7* was amplified from genomic DNA by PCR using the TK5948 and TK5949 primers, digested and ligated into the XbaI-XhoI sites of pRS316 and pRS315, generating pM4326 and pM5283, respectively. pM5283 was subjected to site-specific mutagenesis to generate *sua7* alleles. The TK7848, TK7849, TK7850, TK7851, TK7852 and TK7853 primers were used to generate the pM5287 (E62K), pM5288 (R78C), pM5289 (K190E), pM5290 (K201E), pM5291 (S53P) and pM5292 (G247V) plasmids, respectively.

A 1.9 kb fragment containing *TOA1* was amplified from genomic DNA by PCR using the TK1518 and TK1519 primers, digested and ligated into the BamHI site of pRS316 and pRS315, generating pM5281 and pM5276, respectively. Subsequently, pM5276 was subjected to site-specific mutagenesis to generate *toal* alleles. The TK7845, TK7846, TK7847, TK7856 and TK7857 primers were used to generate the pM5293 (K255A, R257A, K259A), pM5294 (S220A, S225A, S232A), pM5295 (W285A), pM5296 ($\Delta 217-227$) and pM5297 ($\Delta 55-215/+GGSGG$ linker) plasmids, respectively.

A screen for TAND-interacting proteins using the Sos recruitment system

The Sos recruitment system (The CytoTrap™ Two-Hybrid System, Stratagene) (47) was used to identify factor(s) that could interact with TAND or TAF1. pM2718 (pSos-TAND) was used as bait to screen a yeast cDNA library constructed in pM2721. *Saccharomyces cerevisiae* cdc25H (Supplementary Table 1) was co-transformed with pM2718 and the pM2721-based cDNA library, and then plated onto synthetic medium containing 2% glucose. Colonies grown at 25°C were replica-plated onto synthetic medium containing 2% glucose, or 2% galactose and 1% raffinose. Colonies that grew on galactose-containing medium at 37°C were checked by PCR to exclude suppressor genes for *cdc25* (e.g. *CDC25*, *RAS1*, *RAS2*, *SDC25*, *CYR1*, *TPK1*, *TPK2* and *TPK3*), which are frequently isolated as false positives. The candidate plasmids were re-transformed into *S. cerevisiae* cdc25H with pSos (empty plasmid) or pM2718, to confirm TAND dependency. The remaining

candidates were sequenced in order to identify proteins that interacted with TAND.

Protein expression and the GST pulldown assays

His-TBP was expressed in *Escherichia coli* BL21(DE3) (Novagen), as described previously (48). His-HMO1 was expressed in *E. coli* XL1-Blue (Stratagene). Cells were induced with 0.5 mM isopropyl-1-thio- β -D-galactopyranoside (IPTG) and incubated for 24 h at 15°C in 50 ml of LB broth. GST, GST-tagged TAND (6–208 aa), GST-tagged HMO1 and GST-tagged TBP were expressed in *E. coli* XL1-Blue. Cells were induced with 0.4 mM IPTG and incubated for 3 h at 37°C (GST, GST-TAND, GST-HMO1) or at 30°C (GST-TBP) in 50 ml of LB broth. Cultures were harvested and pellets resuspended in 500 μ l of 0.06 M KCl/Buffer PB [20 mM HEPES-KOH pH 7.9, 0.5 mM EDTA, 6 mM MgCl₂, 0.1% Nonidet P-40, 20% (v/v) glycerol, 7 mM 2-mercaptoethanol and 1 mM phenylmethylsulfonyl fluoride (PMSF)]. Following sonication, lysates were clarified by centrifugation and the supernatants subjected to GST pulldown assays without further purification.

To study the interactions between TAND (6–208 aa), TBP and HMO1, a bacterial lysate containing His-HMO1 or His-TBP was mixed with one containing GST-TAND, GST-TBP, GST-HMO1 or GST, in 500 μ l of 0.1 M KCl/Buffer PB, and then incubated at 4°C for 120 min. Following addition of 10 μ l glutathione-Sepharose™ 4B (GE Healthcare Biosciences), the incubation was continued for a further 120 min, at which time the beads were washed three times with 1 ml 0.1 M KCl/Buffer PB. Beads were boiled in SDS sample buffer to elute bound protein, and the eluates were separated using 10% SDS-PAGE, followed by immunoblotting with polyclonal anti-HMO1 and anti-TBP antibodies.

TAP purification

TAP-tagged HMO1 was purified as described previously (49) with minor modifications. A detailed protocol is available upon request.

Immunoblot analyses

Immunoblotting and preparation of polyclonal antibodies directed against TAF1, TAF11 and TBP have been described previously (7,50,51). Polyclonal antibodies directed against HMO1 (aa 1–246) were raised in rabbits using gel-purified His-HMO1 expressed in *E. coli*.

Chromatin immunoprecipitation (ChIP) analyses

ChIP analysis was conducted according to the Hahn laboratory protocol (http://www.fhrc.org/science/labs/hahn/methods/mol_bio_meth/hahnlab_ChIP_method.html), with minor modifications. A detailed protocol is available upon request.

PCR amplification conditions were: 94°C for 1.5 min; 27 cycles of 94°C for 15 s, 55°C for 30 s and 72°C for 30 s and a final extension at 72°C for 7 min. PCR products were separated using 5% non-denaturing PAGE and stained with SYBR Green I (Invitrogen). Each band was

quantified using an LAS-1000 Plus image analyzer (Fuji Film), and the ratio of IP/input was calculated. The PCR primer pairs used to amplify the following genes were: *RPS5*, TK8935/TK9382; *RPS31*, TK4692/TK4625; *RPL10*, TK5031/TK5032; *RPL3*, TK5035/TK5036; *RPL23B*, TK8993/TK8994; *RPL27B*, TK8997/TK8998; *RPL32*, TK8449/TK8450 and the transcribed region of *POL1* (27) (asterisk), TK3506/TK3507.

Northern blot analyses

Northern blot analyses of several endogenous genes were performed as described previously (50). For detection of *ACT1*, *RPS5*, *RPL3*, *RPS31*, *RPL10*, *RPL32*, *HIS4*, *PHO84*, *PHO12* and *GALI*, DNA fragments were amplified by PCR from yeast genomic DNA, purified, and ³²P-labeled using random priming. The PCR primers used for *ACT1*, *RPS5*, *RPL3*, *RPS31*, *RPL10*, *HIS4*, *PHO84* and *PHO12* were described previously (23,43,50). Other primer pairs used were: *RPL32*, TK4446/TK4447; *GALI*, TK253/TK254.

RPL23B, *RPL27B* and 25S rRNA were also detected by northern blot analysis. The probes were generated by 5'-end labeling gene-specific oligonucleotides with [³²P]ATP using the T4 polynucleotide kinase as described previously (23).

Primer extension analyses

Transcription start sites were mapped by primer extension analysis as described previously (52). Extension reactions were conducted using M-MLV reverse transcriptase (TaKaRa) and [³²P]ATP-labeled oligonucleotide primers. All primers were used both as a primer to generate the DNA sequencing ladder and for primer extension reactions. The primers used were: TK3212 (*RPS5*), TK3214 (*ADH1*), TK5414 (*RPL10*), TK7981 (*TEF2*), TK9588 (*RPL32*), TK9430 (*RPS31*), TK9589 (*RPL27B*), TK9590 (*RPL23B*) and TK9591 (*RPS16A*). The cDNA products were analyzed on a 6.5% polyacrylamide DNA sequencing gel. Gels were exposed to imaging plates (BAS2500, Fuji Film) for quantitation and scanning of electrophoretic images.

RESULTS

HMO1 interacts with TFIID

In this study, the Sos recruitment system (SRS) (47) was used to screen for novel proteins that bind to TAND. The Sos system was chosen because it does not depend on transcription, whereas the standard yeast two-hybrid system does (11,53). Temperature-sensitive *S. cerevisiae* *cdc25H* carrying pSos-TAND (1–208 aa) was transformed with the modified pMyr library. After excluding revertants and transformants carrying *CDC25* or *cdc25* suppressor genes, 75 independent clones expressing Myr-tagged fusion proteins were identified for further analysis. These 75 clones included 15 clones carrying the entire *HMO1* coding region and expressing the HMO1 protein. Because the cDNA library was generated using an oligo (dT) primer and all 15 clones were full length, the N-terminal

segment of HMO1 may be critical for interactions with TAND.

The interaction between HMO1 and TAND appears to be specific, because co-transformation with pMyr-HMO1 and pSos-TAND rescues the growth defect of *S. cerevisiae* *cdc25H* at 37°C, while co-transformation with pMyr-HMO1 and pSos (Figure 1A) or pSos-TAF1 (354–817 aa; data not shown) does not. *Saccharomyces cerevisiae* *cdc25H* is also viable at 37°C in the presence of pMyr-HMO1 and pSos-TBP (Figure 1A), suggesting that HMO1 interacts with TBP. In this assay, the strength of the interaction between HMO1 and TAND/TBP is indistinguishable from that of the well-characterized interaction between TAND and TBP (Figure 1A).

Direct binding between HMO1 and TBP was demonstrated using recombinant proteins in GST pulldown assays (Figure 1B, lanes 4 and 8). Using this method, there was no evidence of direct interaction between HMO1 and TAND (Figure 1B, lane 3), suggesting that HMO1 interacts indirectly with TAND. This is consistent with previous studies showing that HMO1 interacts with TAF11 (54) and TAF13 (55,56). We also examined whether HMO1 co-purifies with TFIID. A small amount of TAF1 (~0.01%), TAF11 (~0.01%) and TBP (<0.001%) were recovered with HMO1-TAP purified from cell extracts (Figure 1C). These results suggest that HMO1 regulates transcription of class II genes via an interaction with TFIID.

Genetic interaction between HMO1 and TAND

Because biochemical studies indicate that HMO1 does not interact directly with TAND (Figure 1), we examined whether there is a genetic interaction between these two factors. On rich medium, we compared the growth properties of wild-type, single ($\Delta hmo1$, $\Delta taf1\Delta TAND$) and double ($\Delta hmo1 \Delta taf1\Delta TAND$) deletion mutants (Figure 2A). Previous studies demonstrated that $\Delta hmo1$ strains exhibit slower growth rates than wild-type strains over a wide range of temperatures (21,57). In contrast, our $\Delta hmo1$ strain demonstrated a cold-sensitive growth phenotype (Figure 2A), presumably due to its specific genetic background. A slight (but reproducible) decrease in growth rate was observed when $\Delta hmo1$ was combined with $\Delta taf1\Delta TAND$ [i.e. TAND1 + 2 ($\Delta 2-86$) or TAND1 + 2 + 3 ($\Delta 2-186$)] (Figure 2A).

When an HMO1 expression plasmid was transfected into wild-type and $\Delta taf1\Delta TAND$ strains, the number of transformants appeared to be significantly lower in $\Delta taf1\Delta TAND$ (10–73 aa) than in the wild-type strain (Figure 2B), due to delayed rates of colony formation in the former strain. This strain-specific toxicity was also HMO1-specific, because it was not observed with empty vector (*), or with a plasmid overexpressing an unrelated protein (VTC1). HMO1 was also overexpressed in wild-type and $\Delta taf1\Delta TAND$ mutant strains [TAND1 (8–42 aa), TAND2 (41–73 aa) or both (10–73 aa)] from the *TEF1* and *TDH3* promoters. The results confirmed that HMO1 overexpression is toxic to cells that are deficient in TAND1 (Figure 2C). One interpretation of these data is that HMO1 and TAND1 perform antagonistic roles in

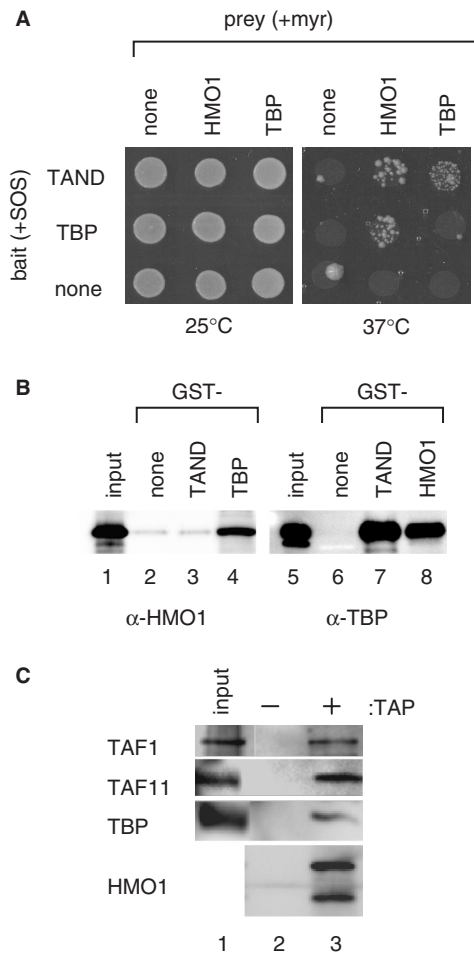


Figure 1. HMO1 interacts with components of TFIID. (A) HMO1 interacts with TAND and TBP in the Sos recruitment system. *Saccharomyces cerevisiae* cdc25H was transformed with the indicated combinations of plasmids and grown on appropriately supplemented 2% galactose and 1% raffinose minimal medium at 25°C (left panel) or 37°C (right panel) for 5 days. Note the revertant colonies (false positives) that did not grow uniformly in inoculated areas. (B) HMO1 binds TBP, but not TAND. GST pull-down assays were performed by incubating HMO1 (200 pmol in lanes 2–4) or TBP (40 pmol in lanes 6–8) with GST-TAND (20 pmol in lanes 3 and 7), GST-TBP (20 pmol in lane 4), GST-HMO1 (25 pmol in lane 8) and GST (60 pmol in lanes 2 and 6). Aliquots of 4% of the total input of HMO1 and TBP are shown in lanes 1 and 5, respectively. Proteins were separated by 10% SDS-PAGE and visualized by immunoblotting using antibodies specific for the proteins indicated. (C) HMO1 co-purifies with TFIID. Cell lysates prepared from strains expressing TAP-tagged or un-tagged HMO1 were purified as described previously (49) with minor modifications. Purified fractions containing TAP-tagged (lane 3) or un-tagged (lane 2) HMO1 were separated by 7% (TAF1), 10% (TAF11) or 12% (HMO1, TBP) SDS-PAGE and visualized by immunoblotting using antibodies against the proteins indicated at the left. TAP-tagged lysates (0.01% of input) are shown in lane 1.

regulating TBP. These genetic data support the hypothesis that HMO1 is involved in transcription of class II genes via its interaction with TBP/TAND1/TFIID.

The effect of $\Delta hmo1$ on TFIID-dependent transcription

To test the hypothesis that HMO1 plays a role in TFIID-dependent transcription, the expression of several

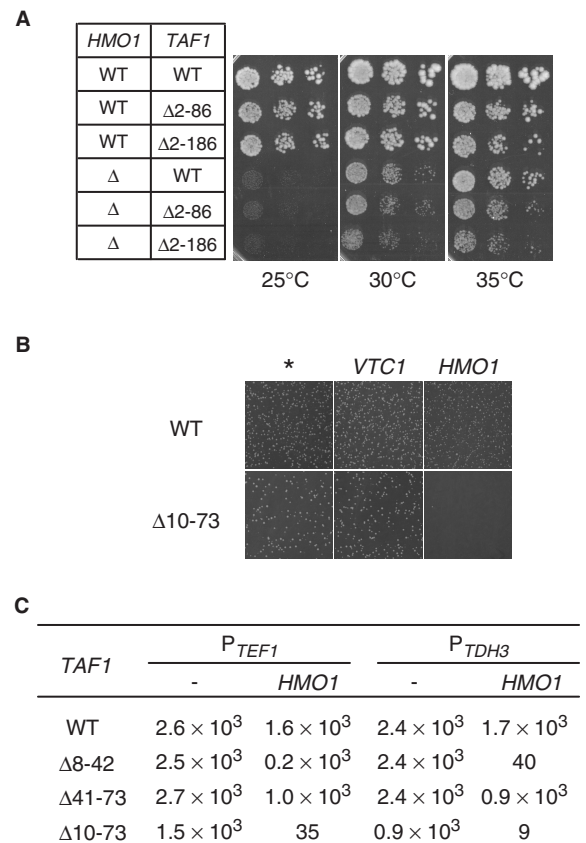


Figure 2. Genetic interaction between HMO1 and TAND. (A) Effect of $\Delta hmo1$ and $taf1\Delta TAND$ on growth. Strains carrying a combination of HMO1 or $\Delta hmo1$ and TAF1, $taf1\Delta TAND$ (2–86 aa) or $taf1\Delta TAND$ (2–186 aa), as indicated at the left, were spotted onto YPD plates at three dilutions and grown at 25°C, 30°C or 35°C for 3 days. (B) The effect of HMO1 overexpression on growth. Strains carrying TAF1 or $taf1\Delta TAND$ (10–73 aa) were transformed with pM2950 or pM2956 to overexpress HMO1 or VTC1, respectively, or with empty plasmid (pM2959, asterisk, negative control). A region of each plate containing transformants cultured at 30°C for 2.5 days is shown. (C) TAND1 or TAND2 are required to reduce the toxicity of HMO1 overexpression. As shown in B, strains carrying TAF1, $taf1\Delta TAND$ (8–42 aa), $taf1\Delta TAND$ (41–73 aa) or $taf1\Delta TAND$ (10–73 aa) were transformed with fixed amounts (100 ng) of empty plasmid (–) or plasmid overexpressing HMO1 (pM2949 and pM2950) from the TEF1 or TDH3 promoters, respectively. Following incubation at 30°C for 2.5 days, the number of transformants were counted.

TAND-dependent genes was examined in wild-type, and in single ($\Delta hmo1$, $taf1\Delta TAND$) or double ($\Delta hmo1 taf1\Delta TAND$) deletion mutants cultured at 25°C, 30°C or 35°C (Figure 3A). As described previously (21), the steady-state levels of 25S rRNA were lower in the $\Delta hmo1$ strain at 25°C and 30°C than in the wild-type strain (compare lanes 1 and 4). Expression of *PHO84*, *PHO12*, *HIS4* and *RPS5* were also HMO1-dependent at 25°C, 30°C and 35°C (compare lanes 1 and 4). In contrast, expression of *ACT1* was relatively HMO1-independent, decreasing significantly only in the $\Delta hmo1 taf1\Delta TAND$ strains at 25°C (compare lanes 2, 3 and lanes 5, 6). Furthermore, expression of *PHO84* was restored in $\Delta hmo1 taf1\Delta TAND$ strains at 35°C (lanes 5 and 6, percentages are indicated in the histogram). The results

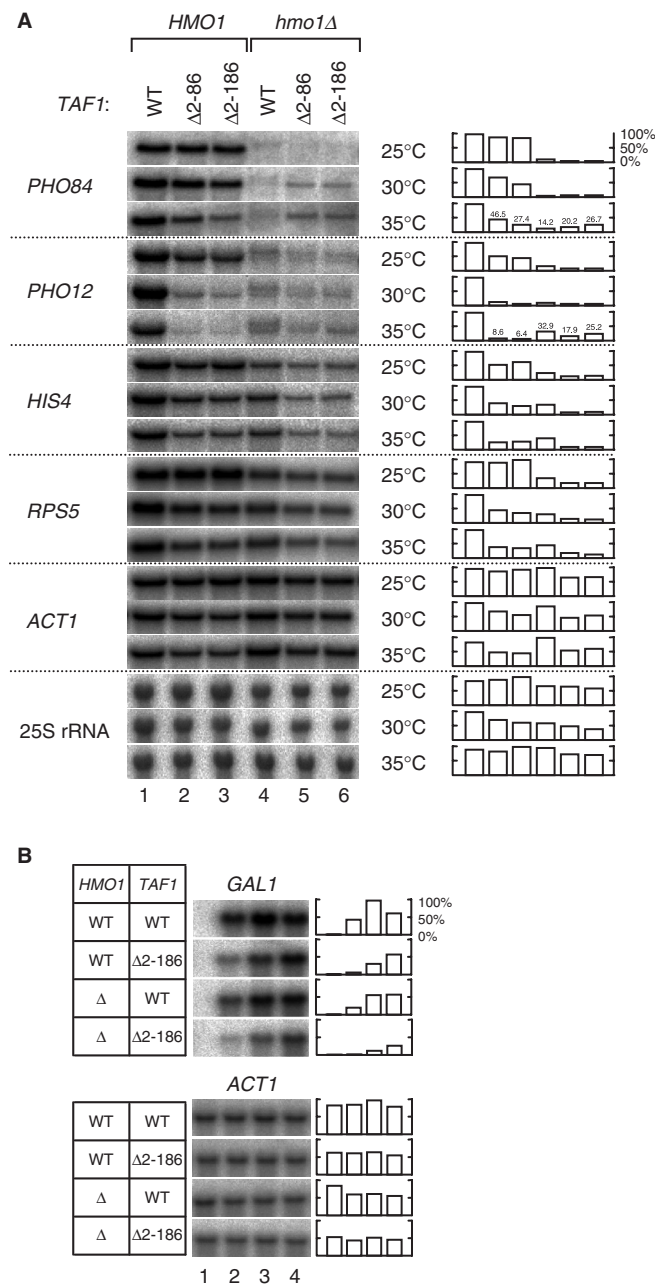


Figure 3. The effect of $\Delta hmo1$ on transcription of class II genes. (A) Transcription of TAND-dependent genes in $\Delta hmo1$ and/or $taf1\Delta TAND$ mutants. Northern blot analysis was used to determine the expression of *PHO84*, *PHO12*, *HIS4*, *RPS5*, *ACT1* and 25S rRNA in the indicated strains. Total RNA (20 μ g) was blotted onto the membrane and hybridized with the gene-specific probes indicated at the left. The raw data (left panel) were quantified and are presented graphically in the right panel. Values for each transcript were normalized to the maximum expression of that transcript. (B) Transcription of an inducible gene in $\Delta hmo1$ and/or $taf1\Delta TAND$ mutants. Expression of *GAL1* (inducible) and *ACT1* (constitutive, control) was measured by northern blot analysis in the indicated strains. Cultures were grown in 3% raffinose synthetic medium to mid-log phase at 30°C, then the same volume of 4% galactose synthetic medium was added and the cultures grown for 3 h at 30°C. Aliquots of the culture were harvested at $t = 0$, 0.5, 1 and 3 h (lanes 1–4, respectively) after addition of galactose. Total RNA was isolated from these samples and then analyzed as described in A.

are consistent with the hypothesis that HMO1 and TAND play antagonistic roles in *PHO84* transcription. A similar, but weaker effect was observed for *PHO12*.

The role of HMO1 in transcription of the inducible *GAL1* gene was also investigated. Here, expression was measured as a function of time after shift from raffinose to galactose-containing medium in wild-type, and in single ($\Delta hmo1$, $taf1\Delta TAND$) or double ($\Delta hmo1 taf1\Delta TAND$) deletion mutant strains (Figure 3B). Deficiency in HMO1 ($\Delta hmo1$) caused a decrease (or delay) in expression of *GAL1*. Deficiency in TAND had a similar but more severe effect, and the effects of these two mutations were additive. These results indicate that HMO1 and TAND function together in *GAL1* transcription. Significantly, mutations in HMO1 and TAND also had additive effects on transcription of *HIS4* and *RPS5* (Figure 3A). Collectively, these data indicate that HMO1 and TAND may regulate transcription of distinct subsets of TFIID-dependent genes in antagonistic or cooperative manners.

The effects of $\Delta hmo1$ and/or $taf1\Delta TAND$ on TFIID occupancy at several RPG promoters

Recent studies have shown that HMO1 binds to many RPG promoters (22,23). We have proposed that 138 RPGs can be classified into 13 distinct groups based on HMO1-abundance at their promoters and the HMO1-dependence of FHL1 and/or RAP1 binding to the promoters (23). For instance, HMO1 is abundant at promoters of *RPS5*, *RPL23B*, *RPL27B* and *RPL32*, but not *RPS31*, *RPL3* and *RPL10* (23). FHL1 binds to the former group in an HMO1-dependent manner, whereas it binds to the latter group in an HMO1-independent manner (23). Intriguingly, however, HMO1-dependence of transcription of these RPGs does not correlate with HMO1 binding or HMO1-dependent recruitment of FHL1 (Figure 4B) (23). Thus, we examined whether TFIID occupancy at these promoters is correlated with the HMO1-dependence of transcription. For this purpose, chromatin immunoprecipitation (ChIP) analyses were conducted in wild-type, and in single ($\Delta hmo1$, $taf1\Delta TAND$) or double ($\Delta hmo1 taf1\Delta TAND$) deletion mutants expressing TAP-tagged TAF1 or TAF1 $\Delta TAND$ that were cultured at 25°C in rich medium (Figure 4A).

The results demonstrate that TFIID occupancy is greater at *RPS5*, *RPS31* and *RPL10* than at *RPL3*, *RPL23B*, *RPL27B* and *RPL32* (Figure 4B), suggesting that TFIID-abundance is not correlated to HMO1-abundance or HMO1-dependent recruitment of FHL1. Intriguingly, $taf1\Delta TAND$ weakened transcription of these RPGs, whereas it enhanced TFIID occupancy at the promoters, irrespective of whether *HMO1* was intact or not (compare open and dark gray bars in Figure 4B). These data are in good agreement with previous results suggesting that TAND is inhibitory for TFIID binding but necessary for efficient transcription (11,51,58).

$\Delta hmo1$ decreased transcription and TFIID occupancy at these promoters in *TAF1* strains (open bars in Figure 4B). However, in $taf1\Delta TAND$ strains, $\Delta hmo1$ decreased transcription of *RPS31*, *RPL3* and *RPL10* but increased TFIID occupancy at these promoters (dark gray

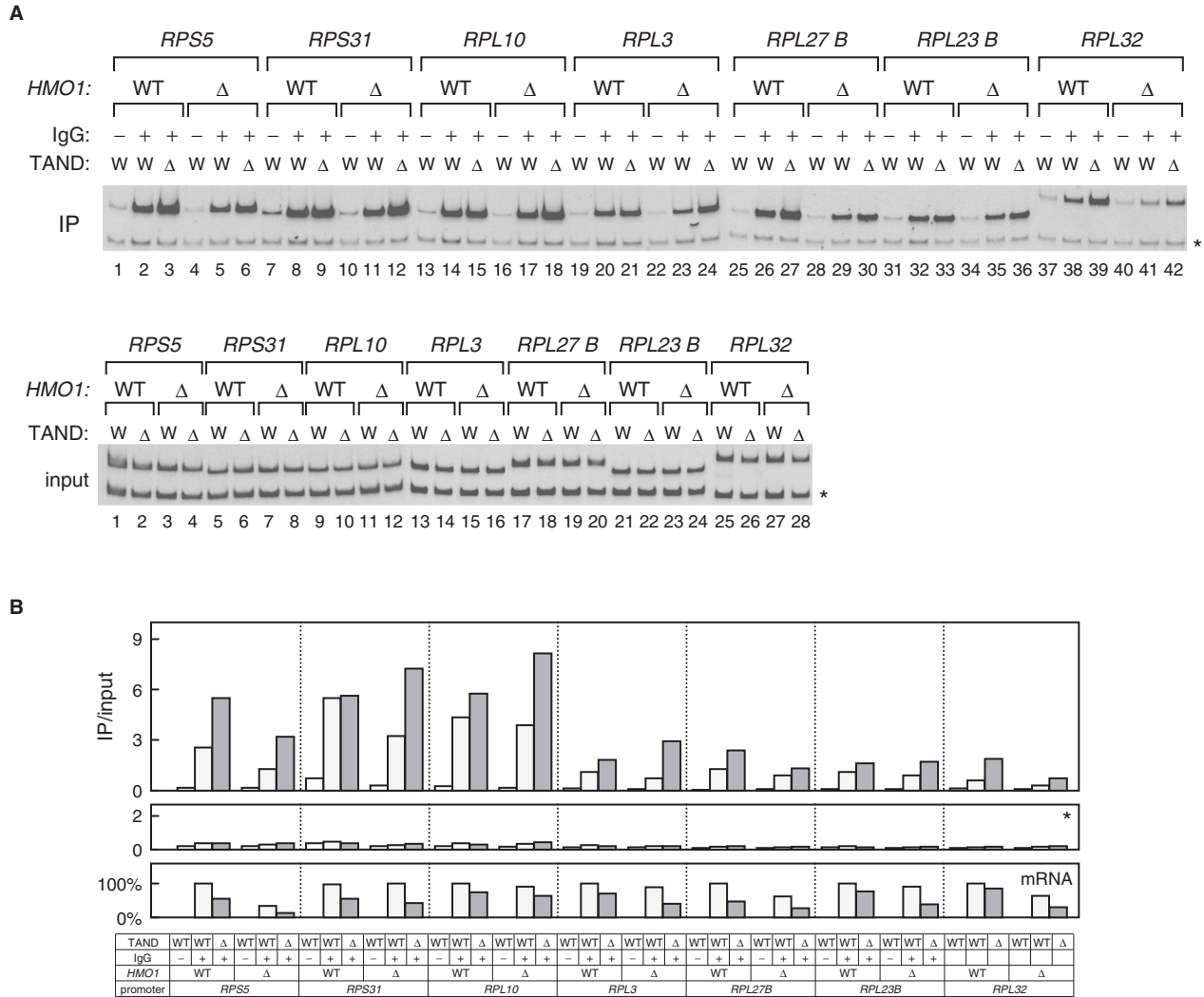


Figure 4. *In vivo* association of TAF1 with RPG promoters. (A) *In vivo* binding of TAF1 to the promoter region of *RPS5*, *RPS31*, *RPL10*, *RPL3*, *RPL27B*, *RPL23B* and *RPL32* was analyzed using ChIP assays. Yeast strains were grown in YPD medium to mid-log phase at 25°C. Cross-linked chromatin from *HMO1* or $\Delta hmo1$ strains expressing TAP-tagged TAF1, with or without the TAF N-terminal domain (TAND; 2–186 aa), as indicated, was prepared and precipitated with either IgG-Sepharose 6 FastFlow (IgG; +) or Sepharose 6 FastFlow (IgG; –, negative control) beads. After reversal of cross-linking, PCR was performed to test for the presence of DNA corresponding to the promoter regions of the indicated genes. Each PCR reaction contained a second primer pair that amplifies a region (218 bp) of the *POL1* ORF as an internal background control (asterisk) (27). The lower panel (input) shows the results of PCR conducted with the chromatin prior to precipitation. (B) Quantitation of the raw data shown in A. Signals corresponding to each band were quantified by an image analyzer after staining with SYBR Green I. The ratio of the precipitated signal (IP) to the input signal from each lysate (table at bottom) was calculated for all the indicated RPG promoters (top panel) as well as for the *POL1* ORF (middle panel). Northern blot analysis was also conducted as described in Figure 3A. The raw data (data not shown) were quantified and are presented graphically in the bottom panel. Values for each transcript were normalized to the maximum expression of that transcript.

bars in Figure 4B). These observations imply that HMO1 may facilitate binding of intact TFIID but inhibit that of TFIID Δ TAND to these promoters. Given that only three of the seven RPGs are HMO1-limited and recruit FHL1 in an HMO1-independent manner (23), HMO1 and TAND/TFIID may function at each RPG promoter in a class-specific manner.

Genetic interaction between HMO1 and TBP, TFIIB, TFIIA

We investigated the genetic relationship between *HMO1* and *SPT15* (TBP; Figure 5A), *SUA7* (TFIIB; Figure 5B)

and *TOA1* (TFIIA; Figure 5C). To construct strains deficient in *SPT15* and/or *HMO1*, plasmids were shuffled in $\Delta spt15$ and $\Delta hmo1 \Delta spt15$ backgrounds. In the newly constructed strains, a *URA3*-marker plasmid expressing *SPT15* was replaced with a *TRP1*-marker plasmid expressing wild-type or mutant *spt15* (39). The viability of these strains was tested at 30°C, 34°C and 37°C in rich medium (Figure 5A). The presence of the $\Delta hmo1$ defect altered the growth of some but not all *spt15* mutant strains. The affected strains were *spt15-E236P*, *K239L*, *F237D*, *K138T/Y139A*, *N159L* and *P65S*, demonstrating an allele-specific genetic interactions between HMO1

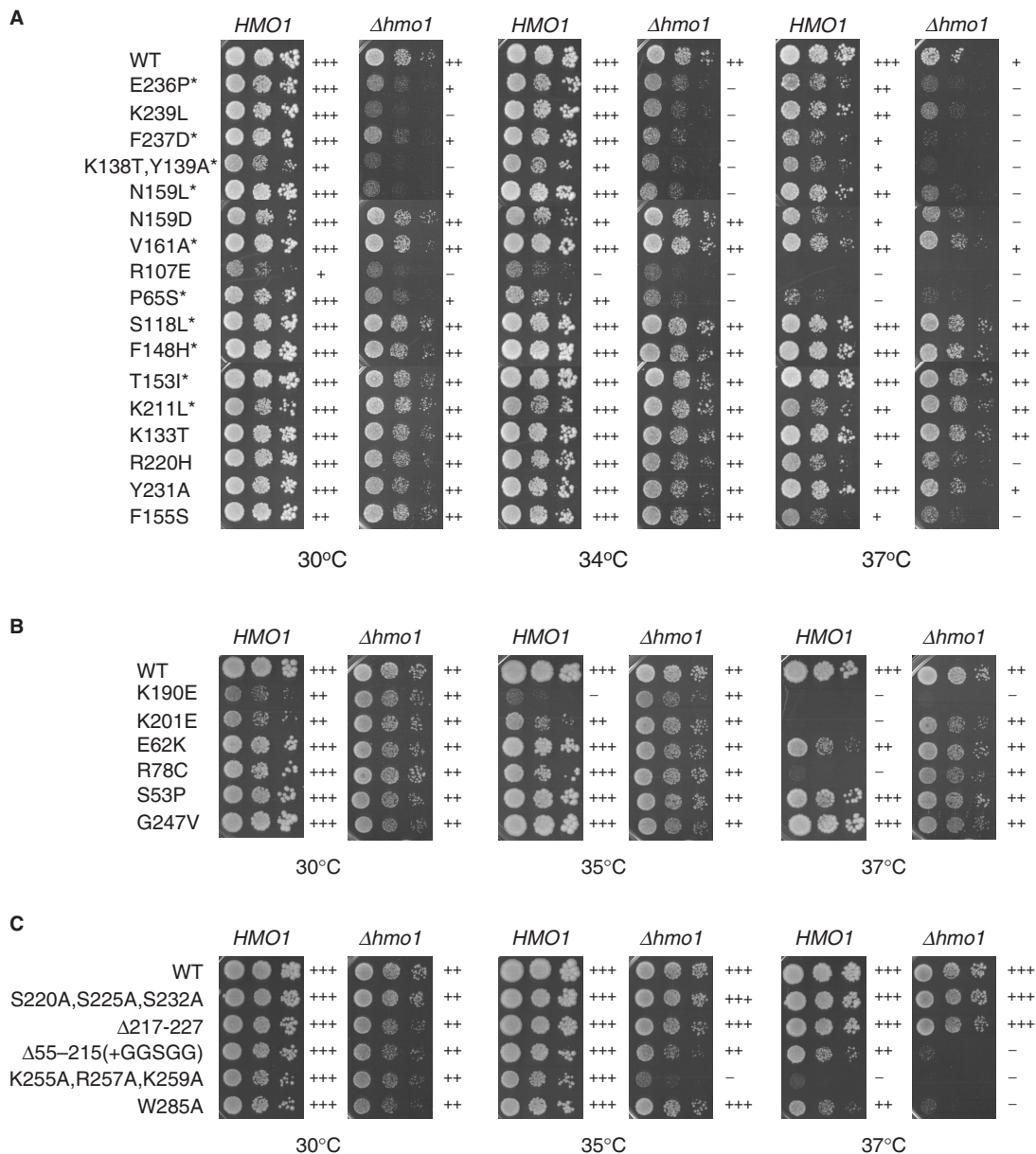


Figure 5. Genetic interaction between *HMO1* and *SPT15*(TBP), *SUA7*(TFIIB), *TOA1*(TFIIA). (A). Effect of $\Delta hmo1$ and *spt15* on growth. The $\Delta spt15$ and $\Delta spt15 \Delta hmo1$ strains carrying plasmid encoding *SPT15* (WT) or *spt15* mutant alleles (indicated at the left) were spotted onto YPD plates at three dilutions and grown for 5 days at the temperatures indicated. Relative growth rates are indicated at the right. Mutants marked with an asterisk are deficient in Pol II-dependent but not Pol I-dependent transcription (59–63). (B) Effect of $\Delta hmo1$ and *sua7* on growth. The $\Delta sua7$ and $\Delta sua7 \Delta hmo1$ strains carrying plasmid encoding *SUA7* (WT) or *sua7* mutant alleles were grown as described in A. (C) Effect of $\Delta hmo1$ and *toal* on growth. The $\Delta toal$ and $\Delta toal \Delta hmo1$ strains carrying plasmid encoding *TOA1* (WT) or *toal* mutant alleles were grown as described in A.

and TBP. Because five of six (all except K239L) of the affected *spt15* mutant alleles are deficient in Pol II-dependent but not Pol I-dependent transcription (59–63), these results indicate that HMO1 may be more intimately involved in the TBP-mediated core promoter function of class II genes than of the 35S rRNA gene. Consistent with this hypothesis, HMO1 binds specifically to the promoter regions of class II genes whereas it binds more broadly to the entire 35S rRNA gene (22,23). The allele-specific interactions between *HMO1* and *SPT15*

suggest a highly specific interaction between these two genes/proteins.

TFIIB mutants were also tested for genetic interactions with $\Delta hmo1$ (Figure 5B). Intriguingly, $\Delta hmo1$ rescued the growth defects of *sua7-K190E* (64), *K201E* (64) and *R78C* (65) at 30/35°C, 30/35/37°C and 37°C, respectively. A similar, but weaker interaction was observed for *sua7-E62K* (65) at 37°C. These results indicate that HMO1 and TFIIB have antagonistic roles, as do HMO1 and TAND (Figures 2B, C and 3A) and

that HMO1 may compete with TFIIB and TAND for binding to TBP.

Similar analyses were performed for several TFIIA mutants (Figure 5C). The results indicate a genetic interaction between $\Delta hmo1$ and *toa1*- $\Delta(55-215)$ (66) (35/37°C), *toa1*-K255A/R257A/K259A (67) (35/37°C) and *toa1*-W285A (68) (37°C). In summary, these results indicate that HMO1 may regulate transcription of class II genes by affecting the formation and/or stability of the TFIIA-TFIIB-TBP/TFIID-promoter complex.

$\Delta hmo1$ restores transcription of class II genes in several *sua7* mutants

The results described above showed that $\Delta hmo1$ reduces the growth of some *spt15* and *toa1* mutants (Figure 5A and C), while it restores the growth of some *sua7* mutants (Figure 5B). Thus, we asked whether the effect of $\Delta hmo1$ on transcription of class II genes is consistent with these growth phenotypes. Indeed, $\Delta hmo1$ impairs transcription of some genes in the *spt15* and *toa1* mutants whereas it restores transcription in the *sua7* mutants.

Northern blot analysis was conducted for the strains described above (Figure 5). The results show that $\Delta hmo1$ significantly reduced the expression of *HIS4* at 25°C and 37°C in the *spt15*-E236P and -K239L mutants (Supplementary Figure 1A). A similar but weaker effect of $\Delta hmo1$ was observed in the *spt15*-F237D and -N159L mutants (Supplementary Figure 1A). In contrast, the *spt15*-K138T/Y139A mutation almost completely abolished *HIS4* expression at both temperatures even in the HMO1 strain (Supplementary Figure 1A). Such a detrimental effect of $\Delta hmo1$ in the *spt15* mutants seems to be specific for a subset of genes since it was observed for *HIS4* but not for *TEF2* (Supplementary Figure 1A), even though HMO1 binds to both promoters at similar levels (23). These results indicate that HMO1 plays different roles in transcription at different promoters.

Consistent with the growth phenotypes, $\Delta hmo1$ restored the expression of *RPS5* at 25°C and 37°C in the *sua7*-K190E and -K201E mutants (Supplementary Figure 1B). A similar but much weaker effect of $\Delta hmo1$ was observed in the *sua7*-E62K and -R78C mutants (Supplementary Figure 1B). Furthermore, $\Delta hmo1$ restored the expression of *HIS4* in the *sua7*-K190E (37°C), -K201E (37°C), -E62K (25/37°C) and -R78C (25/37°C) mutants (Supplementary Figure 1B). $\Delta hmo1$ also restored the expression of *TEF2* in the *sua7*-K190E and -K201E mutants (25/37°C) (Supplementary Figure 1B). Previous studies have shown that the *sua7*-K190E and -K201E mutations are defective in forming a stable TFIIB-TBP-DNA complex while *sua7*-E62K and -R78C mutations shift the transcriptional start site downstream (64,65). Therefore, these results indicate that HMO1 could restore a range of transcriptional defects caused by different types of *sua7* mutations.

Finally, northern blot analyses showed that $\Delta hmo1$ significantly reduced expression of *HIS4* (25/37°C) and *RPS5/TEF2* (25/37°C) in the *toa1*- $\Delta(55-215)$ and *toa1*-W285A mutants, respectively (Supplementary Figure 1B).

Thus, we conclude that the effects of $\Delta hmo1$ on growth and on transcription of a subset of class II genes are well correlated in several *spt15*, *sua7* and *toa1* mutants.

HMO1 participates in start site selection of a subset of class II genes

The results described above indicate that HMO1 and TFIIB function antagonistically in growth and transcription. Since some TFIIB mutants like *sua7*-E62K and -R78C cause a downstream shift in transcriptional start site (64,65), we examined whether $\Delta hmo1$ caused an upstream shift, i.e. a shift in the opposite direction. Transcriptional start sites of *RPS5*, *RPL32*, *RPS31* and *RPL10* were examined by primer extension analysis in some of the strains described in Figure 5B (Figure 6A–D). The electrophoretic images were scanned and quantified to compare the positions of transcriptional start sites (Figure 6E–H). The *sua7*-R78C but not the *sua7*-K190E mutant shifted transcriptional start site of these four genes slightly downstream (compare lanes 1, 3 and 5 in Figure 6A–D), whereas $\Delta hmo1$ alone shifted the transcriptional start site of *RPS5* and *RPL32*, but not of *RPS31* and *RPL10*, upstream (compare lanes 1 and 2 in Figure 6A–D). These results indicate that HMO1 participates in start site selection of a subset of genes. Indeed, a similar upstream shift in transcriptional start site was observed for *RPS16A*, *RPL23B* and *RPL27B*, but not for *TEF2* and *ADH1* (data not shown, Supplementary Figure 2). Notably, $\Delta hmo1$ also shifted the transcriptional start sites of the same set of genes, i.e. *RPS5*, *RPS16A*, *RPL23B*, *RPL27B* and *RPL32*, upstream in the *sua7*-R78C mutant, and less strongly than in the *SUA7* strain (Figure 6A and B, data not shown). In contrast, the upstream shift in transcriptional start sites of these genes induced by $\Delta hmo1$ was quite weak or almost undetectable in the *sua7*-K190E strain (Figure 6A and B, data not shown). Similar results were obtained when the experiments were conducted at different temperatures (i.e. 30°C, 35°C and 37°C) (Supplementary Figure 2, data not shown).

These observations could explain, at least in part, how $\Delta hmo1$ restored the growth of the *sua7*-R78C mutant at 37°C (Figure 5B). Furthermore, given that $\Delta hmo1$ cannot cause a strong upstream shift in the *sua7*-K190E mutant, stable TFIIB-TBP-DNA complex formation must be important for transcriptional initiation from upstream regions. HMO1 is enriched at the promoters of *RPS5*, *RPS16A*, *RPL23B*, *RPL27B* and *RPL32* but limited at those of *RPS31*, *RPL10*, *TEF2* and *ADH1* (23). Therefore, HMO1 may play more direct and important roles in start site selection at HMO1-enriched promoters than at HMO1-limited promoters.

DISCUSSION

In this study, we identified HMO1 as a TAND-interacting protein using the Sos recruitment system (Figure 1A) and showed that HMO1 binds directly to TBP and TFIID (Figure 1B and C). Our evidence suggests that HMO1 may function with TAND either antagonistically or

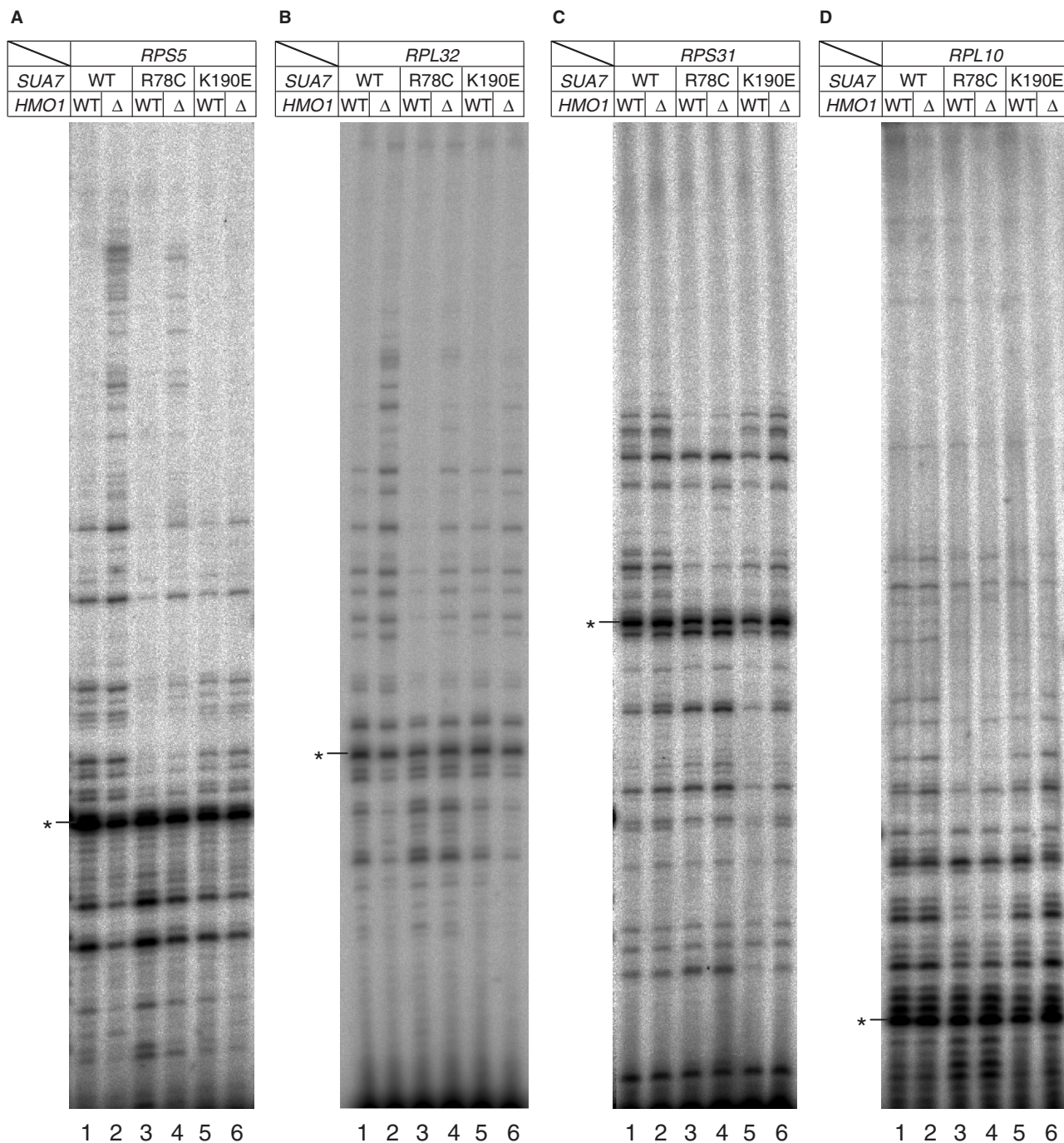


Figure 6. The effect of $\Delta hmo1$ on start site selection of class II genes in *sua7* mutants. (A) Transcriptional start sites of *RPS5* in $\Delta hmo1$ and/or *sua7* mutants. Total RNA (20 μ g) from strains containing the alleles indicated at the top was isolated 2 h after a temperature shift to 37°C from 30°C before being subjected to primer extension analysis. The position of a major transcriptional start site (C at -37 numbered relative to the A (+1) of the start codon ATG) is indicated by the asterisk. (B) Transcriptional start sites of *RPL32* in $\Delta hmo1$ and/or *sua7* mutants. Primer extension analysis was done as described in A. A major transcriptional start site at -365 is indicated by the asterisk. (C) Transcriptional start sites of *RPS31* in $\Delta hmo1$ and/or *sua7* mutants. Primer extension analysis was done as described in A. A major transcriptional start site at -57 is indicated by the asterisk. (D) Transcriptional start sites of *RPL10* in $\Delta hmo1$ and/or *sua7* mutants. Primer extension analysis was done as described in A. A major transcriptional start site at -21 is indicated by the asterisk. (E) Each lane of the electropherogram shown in A was scanned and quantified by densitometry (Multi Gauge ver.3.0, Fuji Film) (*SUA7*, left panel; *sua7-R78C*, center panel; *sua7-K190E*, right panel). The solid and broken lines represent the results obtained from *HMO1* and $\Delta hmo1$ strains, respectively. Asterisks indicate the peaks that correspond to the major transcriptional start sites described in A. The upstream regions were expanded and are shown in the lower panels to make the differences between *HMO1* and $\Delta hmo1$ strains more evident. (F) Each lane of the electropherogram shown in B was scanned and presented as described in E. (G) Each lane of the electropherogram shown in C was scanned and presented as described in E. (H) Each lane of the electropherogram shown in D was scanned and presented as described in E.

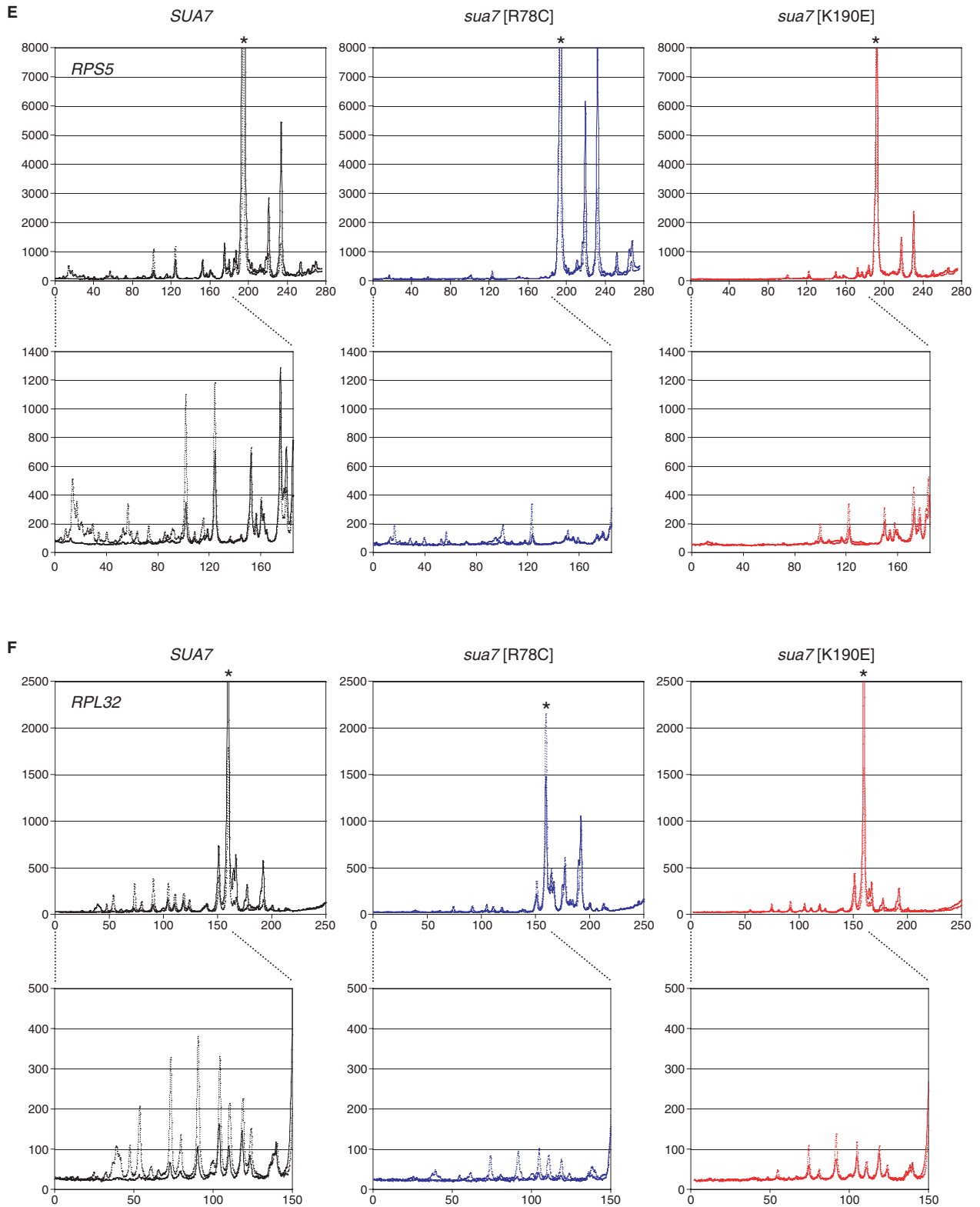


Figure 6. Continued.

cooperatively in supporting cell growth (Figure 2) and transcription of a subset of class II genes (Figure 3). Furthermore, allele-specific interactions of $\Delta hmo1$ with *spt15*, *sua7* and *toal* indicate that HMO1 may be involved

in TFIIA-TFIIB-TBP/TFIID-DNA complex formation (Figure 5, Supplementary Figure 1).

NHP6A/B, another well-characterized HMGB protein in yeast, may also enhance assembly of the

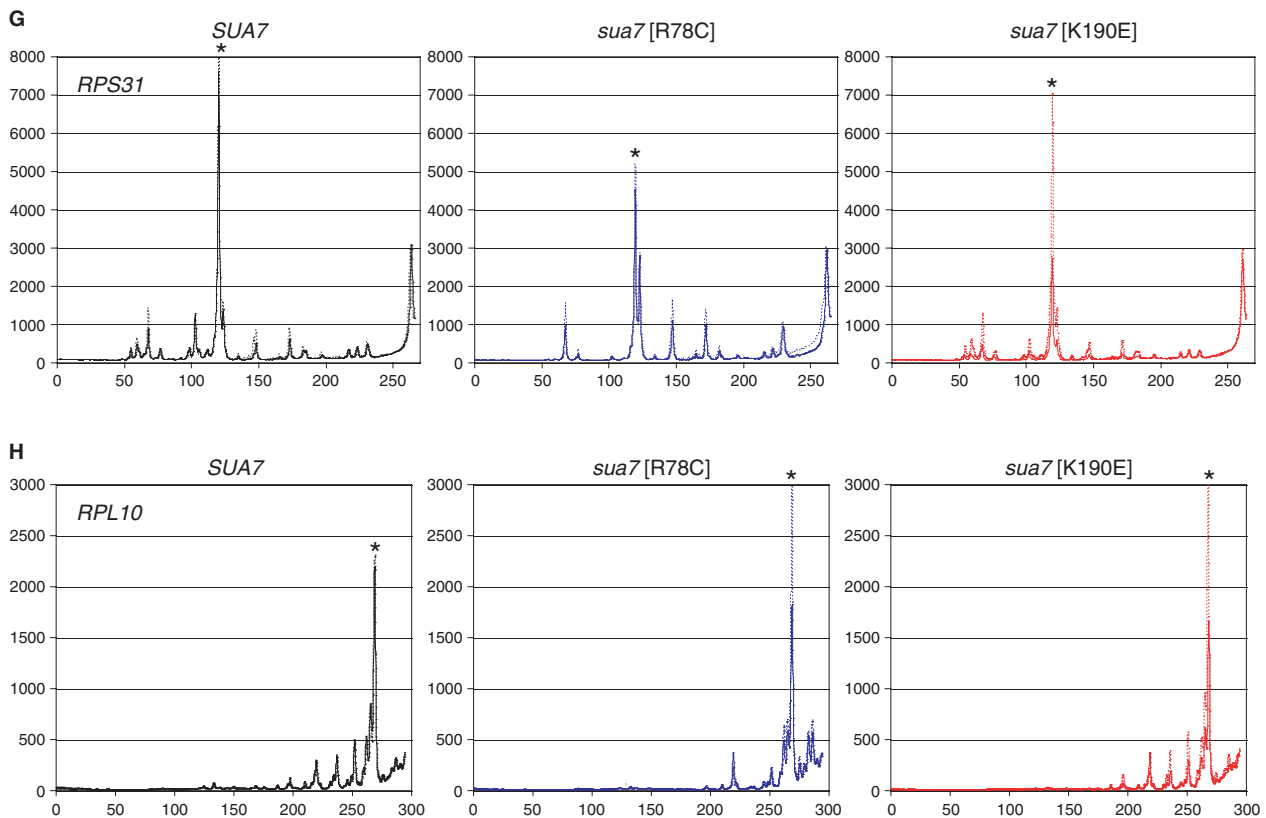


Figure 6. Continued.

TFIIA–TBP–DNA complex (20,69). Does NHP6A/B play a role similar to HMO1 in transcription? Substitutions of TBP residues F237/K239, K138/Y139 or P65 exhibited synthetic growth defects in $\Delta hmo1$ cells (Figure 5A). Similarly, these substitutions were lethal in $\Delta nhp6a/b$ cells (70). However, $\Delta hmo1$ exhibited no apparent synthetic phenotype with $\Delta nhp6a/b$ (57). These results suggest that HMO1 and NHP6A/B are not functionally redundant, but that they may instead have complementary functions, for example, in regulating different subsets of class II genes via similar mechanisms. In fact, each plays a crucial role in Pol I (21) and Pol III (71) transcription, respectively.

$\Delta hmo1$ caused growth defects in some, but not all, of the TBP mutants that are lethal with *taf1* Δ *TAND*. For instance, the TBP mutations N159D, V161A and S118L have growth defects in combination with *taf1* Δ *TAND* (39), but not with $\Delta hmo1$ (Figure 5A). These observations indicate that HMO1 and TAND have both shared and unique functional roles, which is consistent with the observation that the synthetic defect between *taf1* Δ *TAND* and $\Delta hmo1$ is relatively weak (Figure 2A).

One of the most intriguing findings of this study is that $\Delta hmo1$ causes an upstream shift in transcriptional start sites of a subset of genes (Figure 6, data not shown). This phenotype is uncommon and has previously been found in mutations of four polypeptides within the preinitiation complex (PIC), i.e. the TFG1 and TFG2 subunits of TFIIF (31–33) and the RPB2 and RPB9 subunits of Pol II (34–37). Conversely, mutations in the amino-terminal

B-finger region (e.g. residues E62, F63, R64, F66, R78 and V79) of TFIIB (64,65,72) and in the RPB1 subunit (e.g. residues K332, R344 and N445 in the active site) of Pol II (73,74) cause a downstream shift in transcriptional start site. Mutations of *TFG1*, *TFG2*, *RPB2* and *RPB9* could rescue growth defects and suppress the downstream start site shift caused by mutations of *SUA7* (TFIIB) and *RPB1*. Similarly, our current study showed that $\Delta hmo1$ could rescue the growth and transcriptional defects of some TFIIB mutants (Figures 5 and 6, and Supplementary Figure 1). Thus, it will be important in future studies to determine whether $\Delta hmo1$ and mutations of TFIIF/Pol II cause upstream start site shifts by similar or different mechanisms.

The dimerization domain (i.e. the interface between TFG1 and TFG2) of TFIIF and the B-finger of TFIIB lie within the active site of Pol II in the PIC (32,74,75). In contrast, the position of the G369 residue of RPB2, whose mutation causes an upstream start site shift and suppresses the growth and transcriptional defects of the TFIIB mutant, was located near RPB9 but distal to the active site of Pol II (76). However, mutations of *RPB2* and *RPB9* may impair interactions between TFIIF and Pol II (33). Furthermore, a mutation in the switch 2 region of Pol II (i.e. *rpb1-R344A*) that causes a downstream start site shift destabilizes a short RNA–DNA hybrid in the active site and thereby increases the frequency of abortive initiation (74). Based on these and other observations, an intriguing model was recently proposed for the roles

played by the B-finger of TFIIB, TFIIF and the switch 2 region of Pol II (74). In this model, the nascent short RNA–DNA hybrid is initially stabilized by the B-finger of TFIIB, and continued synthesis of RNA induces a conformational change in Pol II, presumably mediated by TFIIF. Subsequently, the switch 2 region is repositioned in the active site to displace the B-finger and then stabilize the 3'-end of the RNA–DNA hybrid. Thus, mutations of the B-finger and switch 2 region that fail to stabilize the RNA–DNA hybrid in the active site would increase the frequency of abortive initiations and result in re-initiation from sites farther downstream. Mutations of TFIIF and Pol II that disrupt the appropriate TFIIF–Pol II interactions may generate an initiation complex that more readily undergoes the conformational change to start transcription from sites farther upstream than normal.

One possible explanation for the phenotypes of $\Delta hmo1$ is that the absence of HMO1 disrupts the appropriate TFIIF–Pol II interactions indirectly, as proposed for *RPB2* and *RPB9* mutants. However, HMO1 may be involved in TFIIA–TFIIB–TBP/TFIID–DNA complex formation, as described above. In addition, the *ADH1* transcriptional start site was shifted in TFIIB, TFIIF, and Pol II mutants, but not in the $\Delta hmo1$ mutant (Supplementary Figure 2). Thus, the alternative hypothesis that the absence of HMO1 may facilitate TFIIA–TFIIB–TBP/TFIID–DNA complex formation at sites farther upstream than normal should be considered. In this regard, it is notable that TBP (SPT15) and several components of SAGA, e.g. SPT3, SPT7, SPT8 and SPT20, were originally isolated as *SPT* genes that suppress Spt- phenotypes, indicating that mutations in TBP or SAGA weakened transcription of the transposon Ty or δ element, but enhanced transcription of adjacent genes (77,78). Although the precise mechanisms by which these mutations could induce a promoter shift from the transposon to an adjacent gene remain unknown, it is likely that TBP binding may be altered to prefer the latter promoter. Hence, it is also possible that $\Delta hmo1$ may alter the site of TBP binding upstream by similar mechanisms.

Recently, NHP6A/B was shown to serve as a Pol III initiation fidelity factor, since $\Delta nhp6a/b$ cells lose initiation fidelity (i.e. generate many ectopic initiation sites) at some, but not all, tRNA genes (79). Biochemical analyses suggest that NHP6A/B may directly promote accurate binding of TFIIB to the correct position, or indirectly via the function of TFIIC. Although HMO1 does not show similar activity in the Pol III system (79), it may play an analogous role in the Pol II system, e.g. by promoting correct binding of TBP/TFIID at a subset of class II gene promoters.

The functions of HMO1 and NHP6A/B in start site selection appear to be promoter-specific (Figure 6, Supplementary Figure 2, data not shown) (79). Notably, the effects of TFIIB and Pol II mutations are also promoter-specific; they shifted transcriptional start sites of *ADH1* and *CYC1* but not of *HIS3* (72,73). Mutation analyses using *ADH1–HIS3* hybrid promoters revealed that the feature that confers sensitivity to TFIIB mutations is encoded in the sequence surrounding the start site

and not by the spacing between the TATA element and the start site (72). Similar but more intricate promoter-specific effects were observed for a E51 mutation (corresponding to E62 in yeast) within the B-finger of human TFIIB; this mutation shifted the transcriptional start site of the AdE4 promoter downstream and that of HIV-LTR upstream, even though it did not affect the transcriptional start sites of AdML and hIGFII promoters (80). Consistent with yeast studies, hybrid promoter analysis showed that these promoter-specific effects were determined by the sequence surrounding the start site (i.e. initiator) (80). Intriguingly, the same mutation shifted transcriptional start site of HIV-LTR downstream (i.e. in the opposite direction) when a single base-pair substitution was introduced at a specific position in the initiator region of this promoter (80). These observations indicate a common mechanism of TFIIB-mediated start site selection that is conserved from yeast to human, although the identity of the human counterpart of HMO1 still remains unclear (21–23).

Our previous study showed that HMO1-abundance and HMO1-dependence of transcription and FHL1-recruitment were determined by the promoter sequence itself, at least in the case of *RPS5* and *RPL10* (23). Thus, the promoter sequence may also determine the sensitivity of start site selection to $\Delta hmo1$. Further studies are required to elucidate the full role played by HMO1 in transcription, and, particularly, in start site selection in RPGs and other HMO1-dependent class II genes.

ACKNOWLEDGEMENTS

We would like to thank Dr H. Iwasaki, Dr T. Kobayashi and members of our laboratory for advice and comments on this work. We also thank Dr A. G. Hinnebusch, Dr Y. Nakatani and Dr J. Heitman for yeast strains, and M. Funk, Y. Ohyama, A. Kobayashi, M. Yuhki, Y. Tsukihashi, S. Takahata, S. Tomita and A. Okada-Marubayashi for plasmids. The TAP plasmid was obtained from CellZome (Heidelberg). This study was supported by a grant from the 2007 Strategic Research Project (No.W19021) of Yokohama City University, and grants from the Japan Society for the Promotion of Science, the Ministry of Education, Culture, Sports, Science and Technology of Japan, CREST of the Japan Science and Technology Corporation, and the Mitsubishi Foundation. Funding to pay the Open Access publication charges for this article was provided by the Japan Society for the Promotion of Science.

Conflict of interest statement. None declared.

REFERENCES

1. Mellor, J. (2005) The dynamics of chromatin remodeling at promoters. *Mol. Cell*, **19**, 147–157.
2. Hahn, S. (2004) Structure and mechanism of the RNA polymerase II transcription machinery. *Nat. Struct. Mol. Biol.*, **11**, 394–403.
3. Taatjes, D.J., Marr, M.T. and Tjian, R. (2004) Regulatory diversity among metazoan co-activator complexes. *Nat. Rev. Mol. Cell Biol.*, **5**, 403–410.

4. Ptashne, M. (2005) Regulation of transcription: from lambda to eukaryotes. *Trends Biochem. Sci.*, **30**, 275–279.
5. Govind, C.K., Yoon, S., Qiu, H., Govind, S. and Hinnebusch, A.G. (2005) Simultaneous recruitment of coactivators by Gen4p stimulates multiple steps of transcription in vivo. *Mol. Cell Biol.*, **25**, 5626–5638.
6. Matangasombut, O., Buratowski, R.M., Swilling, N.W. and Buratowski, S. (2000) Bromodomain factor 1 corresponds to a missing piece of yeast TFIID. *Genes Dev.*, **14**, 951–962.
7. Kotani, T., Miyake, T., Tsukihashi, Y., Hinnebusch, A.G., Nakatani, Y., Kawaichi, M. and Kokubo, T. (1998) Identification of highly conserved amino-terminal segments of dTAFII230 and yTAFII145 that are functionally interchangeable for inhibiting TBP-DNA interactions in vitro and in promoting yeast cell growth in vivo. *J. Biol. Chem.*, **273**, 32254–32264.
8. Kuras, L. and Struhl, K. (1999) Binding of TBP to promoters in vivo is stimulated by activators and requires Pol II holoenzyme. *Nature*, **399**, 609–613.
9. Li, X.Y., Virbasius, A., Zhu, X. and Green, M.R. (1999) Enhancement of TBP binding by activators and general transcription factors. *Nature*, **399**, 605–609.
10. Kim, J. and Iyer, V.R. (2004) Global role of TATA box-binding protein recruitment to promoters in mediating gene expression profiles. *Mol. Cell Biol.*, **24**, 8104–8112.
11. Kotani, T., Banno, K., Ikura, M., Hinnebusch, A.G., Nakatani, Y., Kawaichi, M. and Kokubo, T. (2000) A role of transcriptional activators as antirepressors for the autoinhibitory activity of TATA box binding of transcription factor IID. *Proc. Natl Acad. Sci. USA*, **97**, 7178–7183.
12. Bustin, M. (2001) Revised nomenclature for high mobility group (HMG) chromosomal proteins. *Trends Biochem. Sci.*, **26**, 152–153.
13. Thomas, J.O. and Travers, A.A. (2001) HMG1 and 2, and related 'architectural' DNA-binding proteins. *Trends Biochem. Sci.*, **26**, 167–174.
14. Weir, H.M., Kraulis, P.J., Hill, C.S., Raine, A.R., Laue, E.D. and Thomas, J.O. (1993) Structure of the HMG box motif in the B-domain of HMG1. *EMBO J.*, **12**, 1311–1319.
15. Read, C.M., Cary, P.D., Crane-Robinson, C., Driscoll, P.C. and Norman, D.G. (1993) Solution structure of a DNA-binding domain from HMG1. *Nucleic Acids Res.*, **21**, 3427–3436.
16. Grasser, K.D. (2003) Chromatin-associated HMGA and HMGB proteins: versatile co-regulators of DNA-dependent processes. *Plant Mol. Biol.*, **53**, 281–295.
17. Reeves, R. and Adair, J.E. (2005) Role of high mobility group (HMG) chromatin proteins in DNA repair. *DNA Repair*, **4**, 926–938.
18. Agresti, A. and Bianchi, M.E. (2003) HMGB proteins and gene expression. *Curr. Opin. Genet. Dev.*, **13**, 170–178.
19. Shykind, B.M., Kim, J. and Sharp, P.A. (1995) Activation of the TFIID-TFIIA complex with HMG-2. *Genes Dev.*, **9**, 1354–1365.
20. Paull, T.T., Carey, M. and Johnson, R.C. (1996) Yeast HMG proteins NHP6A/B potentiate promoter-specific transcriptional activation in vivo and assembly of preinitiation complexes in vitro. *Genes Dev.*, **10**, 2769–2781.
21. Gadal, O., Labarre, S., Boschiero, C. and Thuriaux, P. (2002) Hmo1, an HMG-box protein, belongs to the yeast ribosomal DNA transcription system. *EMBO J.*, **21**, 5498–5507.
22. Hall, D.B., Wade, J.T. and Struhl, K. (2006) An HMG protein, Hmo1, associates with promoters of many ribosomal protein genes and throughout the rRNA gene locus in *Saccharomyces cerevisiae*. *Mol. Cell Biol.*, **26**, 3672–3679.
23. Kasahara, K., Ohtsuki, K., Ki, S., Aoyama, K., Takahashi, H., Kobayashi, T., Shirahige, K. and Kokubo, T. (2007) Assembly of regulatory factors on rRNA and ribosomal protein genes in *Saccharomyces cerevisiae*. *Mol. Cell Biol.*, **27**, 6686–6705.
24. Rudra, D., Mallick, J., Zhao, Y. and Warner, J.R. (2007) Potential interface between ribosomal protein production and pre-rRNA processing. *Mol. Cell Biol.*, **27**, 4815–4824.
25. Zhao, Y., McIntosh, K.B., Rudra, D., Schawald, S., Shore, D. and Warner, J.R. (2006) Fine-structure analysis of ribosomal protein gene transcription. *Mol. Cell Biol.*, **26**, 4853–4862.
26. Rudra, D., Zhao, Y. and Warner, J.R. (2005) Central role of Ifh1p-Fhl1p interaction in the synthesis of yeast ribosomal proteins. *EMBO J.*, **24**, 533–542.
27. Wade, J.T., Hall, D.B. and Struhl, K. (2004) The transcription factor Ifh1 is a key regulator of yeast ribosomal protein genes. *Nature*, **432**, 1054–1058.
28. Schawald, S.B., Kabani, M., Howald, I., Choudhury, U., Werner, M. and Shore, D. (2004) Growth-regulated recruitment of the essential yeast ribosomal protein gene activator Ifh1. *Nature*, **432**, 1058–1061.
29. Martin, D.E., Soulard, A. and Hall, M.N. (2004) TOR regulates ribosomal protein gene expression via PKA and the Forkhead transcription factor FHL1. *Cell*, **119**, 969–979.
30. Garbett, K.A., Tripathi, M.K., Cencki, B., Layer, J.H. and Weil, P.A. (2007) Yeast TFIID serves as a coactivator for Rap1p by direct protein-protein interaction. *Mol. Cell Biol.*, **27**, 297–311.
31. Sun, Z.W. and Hampsey, M. (1995) Identification of the gene (SSU71/TFG1) encoding the largest subunit of transcription factor TFIIF as a suppressor of a TFIIB mutation in *Saccharomyces cerevisiae*. *Proc. Natl Acad. Sci. USA*, **92**, 3127–3131.
32. Freire-Picos, M.A., Krishnamurthy, S., Sun, Z.W. and Hampsey, M. (2005) Evidence that the Tfg1/Tfg2 dimer interface of TFIIF lies near the active center of the RNA polymerase II initiation complex. *Nucleic Acids Res.*, **33**, 5045–5052.
33. Ghazy, M.A., Brodie, S.A., Ammerman, M.L., Ziegler, L.M. and Ponticelli, A.S. (2004) Amino acid substitutions in yeast TFIIF confer upstream shifts in transcription initiation and altered interaction with RNA polymerase II. *Mol. Cell Biol.*, **24**, 10975–10985.
34. Chen, B.S. and Hampsey, M. (2004) Functional interaction between TFIIB and the Rpb2 subunit of RNA polymerase II: implications for the mechanism of transcription initiation. *Mol. Cell Biol.*, **24**, 3983–3991.
35. Hull, M.W., McKune, K. and Woychik, N.A. (1995) RNA polymerase II subunit RPB9 is required for accurate start site selection. *Genes Dev.*, **9**, 481–490.
36. Sun, Z.W., Tessmer, A. and Hampsey, M. (1996) Functional interaction between TFIIB and the Rpb9 (Ssu73) subunit of RNA polymerase II in *Saccharomyces cerevisiae*. *Nucleic Acids Res.*, **24**, 2560–2566.
37. Ziegler, L.M., Khapersky, D.A., Ammerman, M.L. and Ponticelli, A.S. (2003) Yeast RNA polymerase II lacking the Rpb9 subunit is impaired for interaction with transcription factor IIF. *J. Biol. Chem.*, **278**, 48950–48956.
38. Amberg, D.C., Burke, D.J. and Strathern, J.N. (2005) *Methods in Yeast Genetics: A Cold Spring Harbor Laboratory Course Manual*, Cold Spring Harbor Laboratory Press, Cold Spring Harbor, NY.
39. Kobayashi, A., Miyake, T., Ohya, Y., Kawaichi, M. and Kokubo, T. (2001) Mutations in the TATA-binding protein, affecting transcriptional activation, show synthetic lethality with the TAF145 gene lacking the TAF N-terminal domain in *Saccharomyces cerevisiae*. *J. Biol. Chem.*, **276**, 395–405.
40. Longtine, M.S., McKenzie, A. III, Demarini, D.J., Shah, N.G., Wach, A., Brachat, A., Philippsen, P. and Pringle, J.R. (1998) Additional modules for versatile and economical PCR-based gene deletion and modification in *Saccharomyces cerevisiae*. *Yeast*, **14**, 953–961.
41. Kokubo, T., Swanson, M.J., Nishikawa, J.I., Hinnebusch, A.G. and Nakatani, Y. (1998) The yeast TAF145 inhibitory domain and TFIIA competitively bind to TATA-binding protein. *Mol. Cell Biol.*, **18**, 1003–1012.
42. Christianson, T.W., Sikorski, R.S., Dante, M., Shero, J.H. and Hieter, P. (1992) Multifunctional yeast high-copy-number shuttle vectors. *Gene*, **110**, 119–122.
43. Takahata, S., Ryu, H., Ohtsuki, K., Kasahara, K., Kawaichi, M. and Kokubo, T. (2003) Identification of a novel TATA element-binding protein binding region at the N terminus of the *Saccharomyces cerevisiae* TAF1 protein. *J. Biol. Chem.*, **278**, 45888–45902.
44. Kasahara, K., Kawaichi, M. and Kokubo, T. (2004) In vivo synthesis of Taf1p lacking the TAF N-terminal domain using alternative transcription or translation initiation sites. *Genes Cells*, **9**, 709–721.
45. Mumberg, D., Muller, R. and Funk, M. (1995) Yeast vectors for the controlled expression of heterologous proteins in different genetic backgrounds. *Gene*, **156**, 119–122.
46. Sikorski, R.S. and Hieter, P. (1989) A system of shuttle vectors and yeast host strains designed for efficient manipulation of DNA in *Saccharomyces cerevisiae*. *Genetics*, **122**, 19–27.

47. Aronheim, A., Zandi, E., Hennemann, H., Elledge, S.J. and Karin, M. (1997) Isolation of an AP-1 repressor by a novel method for detecting protein-protein interactions. *Mol. Cell Biol.*, **17**, 3094–3102.
48. Kokubo, T., Gong, D.-W., Yamashita, S., Horikoshi, M., Roeder, R.G. and Nakatani, Y. (1993) Drosophila 230-kDa TFIID subunit, a functional homolog of the human cell cycle gene product, negatively regulates DNA binding of the TATA box-binding subunit of TFIID. *Genes Dev.*, **7**, 1033–1046.
49. Krogan, N.J., Kim, M., Ahn, S.H., Zhong, G., Kobor, M.S., Cagney, G., Emili, A., Shilatifard, A., Buratowski, S. and Greenblatt, J.F. (2002) RNA polymerase II elongation factors of *Saccharomyces cerevisiae*: a targeted proteomics approach. *Mol. Cell Biol.*, **22**, 6979–6992.
50. Tsukihashi, Y., Miyake, T., Kawaichi, M. and Kokubo, T. (2000) Impaired core promoter recognition caused by novel yeast TAF145 mutations can be restored by creating a canonical TATA element within the promoter region of the TUB2 gene. *Mol. Cell Biol.*, **20**, 2385–2399.
51. Takahata, S., Kasahara, K., Kawaichi, M. and Kokubo, T. (2004) Autonomous function of the amino-terminal inhibitory domain of TAF1 in transcriptional regulation. *Mol. Cell Biol.*, **24**, 3089–3099.
52. Carey, M. and Smale, S.T. (2000) *Transcriptional Regulation in Eukaryotes—Concepts, Strategies, and Techniques*. Cold Spring Harbor Laboratory Press, Cold Spring Harbor, New York.
53. Chang, C., Gonzalez, F., Rothermel, B., Sun, L., Johnston, S.A. and Kodadek, T. (2001) The Gal4 activation domain binds Sug2 protein, a proteasome component, in vivo and in vitro. *J. Biol. Chem.*, **276**, 30956–30963.
54. Uetz, P., Giot, L., Cagney, G., Mansfield, T.A., Judson, R.S., Knight, J.R., Lockshon, D., Narayan, V., Srinivasan, M., Pochart, P. et al. (2000) A comprehensive analysis of protein-protein interactions in *Saccharomyces cerevisiae*. *Nature*, **403**, 623–627.
55. Ito, T., Tashiro, K., Muta, S., Ozawa, R., Chiba, T., Nishizawa, M., Yamamoto, K., Kuhara, S. and Sakaki, Y. (2000) Toward a protein-protein interaction map of the budding yeast: a comprehensive system to examine two-hybrid interactions in all possible combinations between the yeast proteins. *Proc. Natl Acad. Sci. USA*, **97**, 1143–1147.
56. Ito, T., Chiba, T., Ozawa, R., Yoshida, M., Hattori, M. and Sakaki, Y. (2001) A comprehensive two-hybrid analysis to explore the yeast protein interactome. *Proc. Natl Acad. Sci. USA*, **98**, 4569–4574.
57. Lu, J., Kobayashi, R. and Brill, S.J. (1996) Characterization of a high mobility group 1/2 homolog in yeast. *J. Biol. Chem.*, **271**, 33678–33685.
58. Guermah, M., Malik, S. and Roeder, R.G. (1998) Involvement of TFIID and USA components in transcriptional activation of the human immunodeficiency virus promoter by NF-kappaB and Sp1. *Mol. Cell Biol.*, **18**, 3234–3244.
59. Kim, T.K., Hashimoto, S., Kelleher, R.J. III, Flanagan, P.M., Kornberg, R.D., Horikoshi, M. and Roeder, R.G. (1994) Effects of activation-defective TBP mutations on transcription initiation in yeast. *Nature*, **369**, 252–255.
60. Lee, M. and Struhl, K. (1995) Mutations on the DNA-binding surface of TATA-binding protein can specifically impair the response to acidic activators in vivo. *Mol. Cell Biol.*, **15**, 5461–5469.
61. Stargell, L.A. and Struhl, K. (1995) The TBP-TFIIA interaction in the response to acidic activators in vivo. *Science*, **269**, 75–78.
62. Stargell, L.A. and Struhl, K. (1996) A new class of activation-defective TATA-binding protein mutants: evidence for two steps of transcriptional activation in vivo. *Mol. Cell Biol.*, **16**, 4456–4464.
63. Schultz, M.C., Reeder, R.H. and Hahn, S. (1992) Variants of the TATA-binding protein can distinguish subsets of RNA polymerase I, II, and III promoters. *Cell*, **69**, 697–702.
64. Bangur, C.S., Pardee, T.S. and Ponticelli, A.S. (1997) Mutational analysis of the D1/E1 core helices and the conserved N-terminal region of yeast transcription factor IIB (TFIIB): identification of an N-terminal mutant that stabilizes TATA-binding protein-TFIIB-DNA complexes. *Mol. Cell Biol.*, **17**, 6784–6793.
65. Pinto, I., Wu, W.H., Na, J.G. and Hampsey, M. (1994) Characterization of sua7 mutations defines a domain of TFIIB involved in transcription start site selection in yeast. *J. Biol. Chem.*, **269**, 30569–30573.
66. Kang, J.J., Auble, D.T., Ranish, J.A. and Hahn, S. (1995) Analysis of the yeast transcription factor TFIIA: distinct functional regions and a polymerase II-specific role in basal and activated transcription. *Mol. Cell Biol.*, **15**, 1234–1243.
67. Ranish, J.A., Yudkovsky, N. and Hahn, S. (1999) Intermediates in formation and activity of the RNA polymerase II preinitiation complex: holoenzyme recruitment and a postrecruitment role for the TATA box and TFIIB. *Genes Dev.*, **13**, 49–63.
68. Solow, S.P., Lezina, L. and Lieberman, P.M. (1999) Phosphorylation of TFIIA stimulates TATA binding protein-TATA interaction and contributes to maximal transcription and viability in yeast. *Mol. Cell Biol.*, **19**, 2846–2852.
69. Biswas, D., Imbalzano, A.N., Eriksson, P., Yu, Y. and Stillman, D.J. (2004) Role for Nhp6, Gen5, and the Swi/Snf complex in stimulating formation of the TATA-binding protein-TFIIA-DNA complex. *Mol. Cell Biol.*, **24**, 8312–8321.
70. Eriksson, P., Biswas, D., Yu, Y., Stewart, J.M. and Stillman, D.J. (2004) TATA-binding protein mutants that are lethal in the absence of the Nhp6 high-mobility-group protein. *Mol. Cell Biol.*, **24**, 6419–6429.
71. Kruppa, M., Moir, R.D., Kolodrubetz, D. and Willis, I.M. (2001) Nhp6, an HMG1 protein, functions in SNR6 transcription by RNA polymerase III in *S. cerevisiae*. *Mol. Cell*, **7**, 309–318.
72. Faltar, S.L., Brodie, S.A. and Ponticelli, A.S. (2001) Promoter-specific shifts in transcription initiation conferred by yeast TFIIB mutations are determined by the sequence in the immediate vicinity of the start sites. *Mol. Cell Biol.*, **21**, 4427–4440.
73. Berroteran, R.W., Ware, D.E. and Hampsey, M. (1994) The sua8 suppressors of *Saccharomyces cerevisiae* encode replacements of conserved residues within the largest subunit of RNA polymerase II and affect transcription start site selection similarly to sua7 (TFIIB) mutations. *Mol. Cell Biol.*, **14**, 226–237.
74. Majovski, R.C., Khapersky, D.A., Ghazy, M.A. and Ponticelli, A.S. (2005) A functional role for the switch 2 region of yeast RNA polymerase II in transcription start site utilization and abortive initiation. *J. Biol. Chem.*, **280**, 34917–34923.
75. Bushnell, D.A., Westover, K.D., Davis, R.E. and Kornberg, R.D. (2004) Structural basis of transcription: an RNA polymerase II-TFIIB cocrystal at 4.5 Angstroms. *Science*, **303**, 983–988.
76. Cramer, P., Bushnell, D.A. and Kornberg, R.D. (2001) Structural basis of transcription: RNA polymerase II at 2.8 angstrom resolution. *Science*, **292**, 1863–1876.
77. Winston, F. and Sudarsanam, P. (1998) The SAGA of Spt proteins and transcriptional analysis in yeast: past, present, and future. *Cold Spring Harb. Symp. Quant. Biol.*, **63**, 553–561.
78. Yamaguchi, Y., Narita, T., Inukai, N., Wada, T. and Handa, H. (2001) SPT genes: key players in the regulation of transcription, chromatin structure and other cellular processes. *J. Bio. Chem.*, **129**, 185–191.
79. Kassavetis, G.A. and Steiner, D.F. (2006) Nhp6 is a transcriptional initiation fidelity factor for RNA polymerase III transcription in vitro and in vivo. *J. Biol. Chem.*, **281**, 7445–7451.
80. Fairley, J.A., Evans, R., Hawkes, N.A. and Roberts, S.G. (2002) Core promoter-dependent TFIIB conformation and a role for TFIIB conformation in transcription start site selection. *Mol. Cell Biol.*, **22**, 6697–6705.